# Carbon and silica megasink in deep-sea sediments of the Congo terminal lobes

Christophe Rabouille, B. Dennielou, François Baudin, Mélanie Raimonet, L. Droz, A. Khripounoff, P. Martinez, L. Mejanelle, P. Michalopoulos, L. Pastor, et al.

# Carbon and silica megasink in deep-sea sediments of the Congo terminal lobes

**C. Rabouille[1*], B. Dennielou[2], F. Baudin[3], M. Raimonet[4], L. Droz[5], A. Khripounoff[6], P. Martinez[7], L. Mejanelle[8], P. Michalopoulos[9], L. Pastor[6], A. Pruski[8], O. Ragueneau[4], J-L. Reyss[1], L. Ruffine[2], J. Schnyder[3], E. Stetten[3], M. Taillefert[10], J. Tourolle[6] and K. Olu[6]**

[1]Laboratoire des Sciences du Climat et de l'Environnement, UMR CEA-CNRS-UVSQ 8212 et IPSL, Université Paris-Saclay, Avenue de la Terrasse, 91190 Gif sur Yvette, France
[2]Unité de Recherche Géosciences Marines, IFREMER, 29280 Plouzané, France
[3]Institut des Sciences de la Terre de Paris, Sorbonne Université, CNRS, UMR 7193, 4 Place Jussieu, 75005 Paris, France
[4]Laboratoire des sciences de l'Environnement Marin, UMR UBO-CNRS, Institut Universitaire Européen de la Mer, 29280 Plouzané, France
[5]Laboratoire Domaines Océaniques, UMR UBO-CNRS6538, Institut Universitaire Européen de la Mer, 29280 Plouzané, France
[6]IFREMER Centre Bretagne, Unité de Recherche Etude des Ecosystèmes Profonds, (REM-EEP-LEP), 29280 Plouzané, France
[7]Environnements et Paléoenvironnements Océaniques et Continentaux, Université de Bordeaux, UMR 5805, Allée Geoffroy St Hilaire, 33615 Pessac Cedex, France
[8]Laboratoire d'Ecogéochimie des Environnements Benthiques, Sorbonne Université, CNRS, UMR 8222, Observatoire Océanologique, 66650 Banyuls-sur-Mer, France
[9] Institute of Oceanography, Hellenic Center for Marine Research, 46.7 km Athens-Sounion An, Anavyssos, 19013, Greece
[10]School of Earth and Atmospheric Sciences, Georgia Institute of Technology, 311 Ferst Dr., Atlanta, GA 30332, USA

Corresponding author: Christophe Rabouille (rabouill@lsce.ipsl.fr) Orcid : https://orcid.org/0000-0003-1211-717X

## Key Points:

- Sediments located at the termination of Congo Canyon and channel-levee system are a large sink of organic carbon (0.35 TgC/yr) and amorphous silica (0.11 TgSi/yr)
- These sediments collect and store in the deep-sea (~5 km depth) 18 and 35% of Congo River organic carbon and amorphous silica inputs, respectively
- Organic carbon burial in these sediments increases OC burial in the entire South Atlantic deep basin (>3000m) by 19% for a surface area <0.01%

- Burial efficiencies in these megasinks are 85% for OC and 73% for aSi

**Keywords:**

Present; Paleoceanography; South Atlantic; Inorganic geochemistry; Organic geochemistry; Sedimentology-marine cores;

## Abstract

Carbon and silicon cycles at the Earth surface are linked to long-term variations of atmospheric $CO_2$ and oceanic primary production. In these cycles, the river-sea interface is considered a biogeochemical hotspot, and deltas presently receive and preserve a major fraction of riverine particles in shallow water sediments. In contrast, periods of glacial maximum lowstand were characterized by massive exports of sediments to the deep-sea via submarine canyons and accumulation in deep-sea fans. Here, we calculate present-day mass balances for organic carbon (OC) and amorphous silica (aSi) in the terminal lobe complex of the Congo River deep-sea fan as an analog for glacial periods. We show that this lobe complex constitutes a megasink with the current accumulation of 18 and 35% of the OC and aSi river input, respectively. This increases the estimates of organic carbon burial by 19% in the South Atlantic Ocean in a zone representing less than 0.01% of the basin. These megasinks might have played a role in carbon trapping in oceanic sediments during glacial times.

## 1 Introduction

The carbon cycle regulates atmospheric $CO_2$ concentration, the major driver of climate variations over different timescales (Cox et al., 2000; Frank et al., 2010; Parrenin et al., 2013). Over the last

64 decade, the coastal ocean, and particularly large river estuaries and deltas, have received
65 increased attention as a biogeochemical hotspot at the interface between the oceanic and
66 continental carbon cycles (Battin et al., 2009; Bauer et al., 2013; Bianchi et al., 2014; Regnier et
67 al., 2013). The silicon cycle is tightly linked to the carbon cycle (Tréguer et al., 2018) with
68 diatom production and export largely contributing to the biological carbon pump and the transfer
69 of particulate carbon from the surface to the deep ocean (Ragueneau et al., 2002). The major
70 role of continent-ocean transfer in the marine silicon cycle has also been recognized (Tréguer
71 and De La Rocha, 2013). As these two cycles are largely intertwined, it is of prime importance to
72 investigate their interaction at the continent-ocean interface (Demaster, 2002; Laruelle et al.,
73 2009).

74 Eustatic sea-level change is a major forcing on continent-ocean sediment transfer and submarine
75 deep-sea fan development as it controls the location of sediment deposition on the shelf during
76 highstands or its delivery to the deep ocean during lowstands (Posamentier and Vail, 1988;
77 Shanmugam and Moiola, 1982; Vail et al., 1977). Though a strict lowstand model of submarine
78 fan development is frequently discussed (Allin et al., 2017; Covault and Graham, 2010; Covault
79 and Fildani, 2014), sea level remains the main control in areas characterized by a large
80 continental shelf like for the Amazon fan (Flood and Piper, 1997), Mississippi (Bouma et al.,
81 1989), Rhone fan (Lombo Tombo et al., 2015) or Danube fan (Constantinescu et al., 2015). In
82 the present highstand ocean, terrestrial particulate organic carbon (OC) and amorphous silica
83 (aSi) are mainly buried and recycled in river deltas (Berner, 1989; Bianchi and Allison, 2009;
84 Bianchi et al., 2014; Blair and Aller, 2012; Burdige, 2005; Hedges and Keil, 1995; Lansard et al.,
85 2009) and continental shelves (80-90%; (Rabouille et al., 2001), and a small fraction of riverine
86 OC and aSi is therefore transported away to continental slopes or the abyssal plain (Canals et al.,

2006; Rabouille et al., 2009). In contrast, a larger fraction of continental carbon and silicon was transferred into canyons connected to rivers during glacial period lowstands, as rivers discharged closer to shelf breaks and slopes (Schlünz et al., 1999; Tsandev et al., 2010). As a result, the exposed continental shelf of the Amazon (Goni, 1997; Keil et al., 1997) or the Mississippi (Burdige, 2005; Newman et al., 1973) was bypassed, and deep-sea fans acted as main carbon and silicon repository during the glacial period. However, these deep-sea repositories are presently inactive making impossible to understand lowstand source-to-sink processes for OC and aSi.

The Congo River is the world's second largest river by its discharge and ranks fifth by its particulate organic carbon input to the ocean (Milliman, 1991; Spencer et al., 2014). It is the only major river directly connected to an active canyon enabling a large amount of its sediment load to bypass the shelf and to be conveyed through the canyon to the deep-sea channel-levees by turbidity current (Babonneau et al., 2002; Dennielou et al., 2017). This direct transfer thereby makes the repository zone named Congo terminal lobes (Mulder and Etienne, 2010; Savoye et al., 2009) excellent analogs to understand the functioning and the significance of river-sea fluxes of carbon and silicon in a lowstand ocean. Indeed, a large and unknown fraction of the 1.9 Tg OC $y^{-1}$ (1Tg =$10^{12}$ g) and 0.33 Tg aSi $y^{-1}$ exported by the Congo River into the Atlantic Ocean is presently transported by turbidity currents over 1000 km along the submarine canyon and deep-sea channel (Azpiroz-Zabala et al., 2017; Khripounoff et al., 2003; Vangriesheim et al., 2009). Previous estimations of the organic carbon and amorphous silica accumulation in the Congo lobe complex (Rabouille et al., 2009; Raimonet et al., 2015; Stetten et al., 2015) lacked a detailed survey of the lobe complex morphology, accurate sedimentation rates, and estimates of the surface area involved to precisely determine the fate of OC and aSi. In this paper, we use a multidisciplinary dataset including detailed remotely operated vehicles (ROV) mapping,

sediment characteristics and composition together with sedimentation rates over the last century, *in situ* benthic chamber fluxes, and sediment traps to quantify the fate of deposited OC and aSi in the Congo lobe complex. This leads to the calculation of a mass balance (burial and recycling) of terrestrial OC and aSi for the lobe complex. We further estimate the proportion of terrestrial amorphous silica and organic carbon from the Congo River trapped in the terminal lobes sink and the importance of this previously unknown C and Si sink in the South Atlantic Ocean for the present and extrapolate to the glacial periods.

## 2. Materials and Methods

### 2.1. Location and background

The present Congo fan lobe complex includes five successive amalgamated lobes developed during the last 4000 years (Dennielou et al., 2017; Picot, 2015). Annual and powerful turbidity currents feeding the lobe complex have been recorded and monitored in the canyon (Heezen et al., 1964) and the deep-sea channel (Azpiroz-Zabala et al., 2017; Khripounoff et al., 2003; Vangriesheim et al., 2009), but the flux of sediment to the lobe complex is difficult to estimate because of the pulsed and unpredictable nature of these turbidity currents. Sediments record the deposition of these currents as exemplified by the counting of turbidites in sediment cores from the lobe complex combined with $^{210}$Pb chronology which shows that the recurrence time of deposits by turbidity currents ranges between 6 and 17 years (Dennielou et al., 2017; Picot, 2015).

### 2.2. Methods for mass balance

Two expeditions were carried out in February 2011 (Olu, 2011) and December 2011 (Rabouille, 2011). State of the art methods were used for assessing mass balances in the terminal lobes of the Congo deep-sea fan. Most data were already published in several papers (see section 3 for references) except sediment trap fluxes, DSi benthic fluxes and aSi sediment content (methods in Supplementary Material). Recycling rates of OC and aSi were calculated from *in situ* measurements of total oxygen uptake (TOU) and dissolved silica (DSi) benthic fluxes with a benthic chamber lander (Khripounoff et al., 2006). Uncertainty on TOU values was calculated from variability among 3 chambers during the same deployment (5-10%) and was propagated as relative uncertainty to the DSi flux. In order to recalculate OC mineralization rates, a $C/O_2$ ($C/O_2$ = 1-2*N/C; Van Cappellen and Wang, 1996) molar ratio of 0.9 was used corresponding to the average observed C/N of 15-20 observed in the area (Stetten et al., 2015). The aSi dissolution rates were assumed similar to measured dissolved silica fluxes. Burial was estimated by multiplying the measured sedimentation rates by porosity and the organic carbon or amorphous silica content (Congolobe group et al., 2017; Stetten et al., 2015; Raimonet et al., 2015) with an uncertainty calculated using 30% variability on sedimentation rates and 5% for the average OC (Baudin et al., 2017a; Baudin et al., 2017b; Stetten et al., 2015) or aSi (Raimonet et al., 2015) concentrations (see Supplementary Material for details) . Vertical fluxes of OC and aSi were measured in 2011 (unpublished data) using sediment traps deployed at 35 m above sea floor for a year at the Congolobe site without any noticeable turbidity current (Supplementrary Material). Therefore, sediment traps have measured the ambient "non-turbiditic" vertical flux. Another sediment trap array was deployed in a nearby site in 2003-2004 (site Bio-D, 200 km east of the lobe complex; Rabouille et al., 2009). In addition, a particular effort was made to estimate the

153 lobe complex perimeter and surface areas of the five lobes using multibeam acoustic backscatter
154 and sub-bottom profiler imagery (Dennielou et al., 2017; and Supplementary Materials).

155 In this paper, we used the classical method for calculating the input of OC and aSi to the lobe
156 complex by summing independent estimates of recycling and burial fluxes (Burdige, 2006):

157 Input to the lobe complex = recycling flux + burial flux (Eq. 2)

158 As sedimentation rates were calculated from $^{210}$Pb chronologies, covering a period of time of
159 about a century (Congolobe group, 2017), the burial timescale encompasses several turbidity
160 events (return time of 6-17 years), and is thus a fair estimate of average burial. Furthermore,
161 since turbiditic activity in the lobe zone was absent throughout 2011 as recorded by sediment
162 traps, we can reasonably assume that recycling is not biased by a pulse input of new turbiditic
163 material and fairly reflects recycling between turbidity events. The OC and aSi total input fluxes
164 were thus computed using the sum of recycling and burial fluxes for each lobe multiplied by its
165 surface area. They were summed to determine the total inputs of OC and aSi to the lobe
166 complex.

167

168 **3 Results: cycling and burial fluxes in the terminal lobe system**

169 3.1 Recycling of OC and aSi derived from benthic chamber measurements

170 TOU and DSi fluxes ranged between 5.4 and 9.6 mmol $O_2$ $m^{-2}$ $d^{-1}$ and between 0.6 and 1.9 mmol
171 Si $m^{-2}$ $d^{-1}$ respectively at the different stations along the lobe complex (Table 1; Olu et al., 2017;
172 Raimonet et al., 2015). TOU fluxes were up to one order of magnitude higher than those
173 recorded in the South Atlantic tropical abyssal plain (0.5-1 mmol $O_2$ $m^{-2}$ $d^{-1}$; Wenzhöfer and

174 Glud, 2002), whereas the DSi fluxes were comparable to fluxes measured in the Equatorial
175 Atlantic (Ragueneau et al., 2009).

176 3.2 Burial flux of OC and aSi in terminal lobe complex sediments

177 High sedimentation rates due to the deposition of turbidites (0.5-1 cm $y^{-1}$; Congolobe group et
178 al., 2017; Rabouille et al., 2009) were recorded over the entire lobe complex. The feeding
179 channel of lobe 5 (the most distal and recent lobe) displayed sedimentation rate of 12 cm $y^{-1}$
180 (Table 1). The sedimentation rates were on average three to four orders of magnitude higher than
181 those in the surrounding abyssal plain (Congolobe group et al., 2017; Mollenhauer et al., 2004;
182 Stetten et al., 2015). The lobe complex sediments were characterized by large OC concentrations
183 of OC (Stetten et al., 2015; Baudin et al., 2017b), exceeding 3% as compared to 0.5% in the
184 Atlantic sediments of the central basin (Mollenhauer et al., 2004). In turn, aSi concentrations
185 (0.9-1.3% Si dry weight; Raimonet et al., 2015) were in the same range as those in the abyssal
186 plain sediments of Eastern Equatorial Atlantic (Ragueneau et al., 2009). As recently proposed by
187 Rahman et al. (2016), aSi concentrations in lobe sediments may have been underestimated by a
188 factor of 2-3, because of amorphous silica alteration in the shelf repository (canyon head) before
189 being entrained by turbidity current. Burial of OC and aSi in terminal lobe sediments showed
190 extremely large fluxes of 38-1560 g C $m^{-2}$ $y^{-1}$ for OC burial and 11-381 g Si $m^{-2}$ $y^{-1}$ for aSi
191 (Table 1). These fluxes exceeded South Atlantic Basin values at these depths (>3000m) by a
192 factor of 2000 for OC (0.06 g C $m^{-2}$ $y^{-1}$; Mollenhauer et al., 2004) and 100 for aSi (maximum 0.4
193 g Si $m^{-2}$ $y^{-1}$; Geibert et al., 2005). OC and aSi burial fluxes were the highest in the feeding
194 channel of lobe 5 (station C, Fig. 1), where sedimentation rates are highest (12 cm $y^{-1}$;
195 Congolobe group et al., 2017). The OC/aSi molar ratios in buried particles (average 7.1) were

196 also consistently high (Table 1), with values that are five times larger than the maximal ratio
197 measured in deep-sea sediments (0.02-1.7; Ragueneau et al., 2002).

198 3.3 Vertical flux of OC and aSi from sediment traps

199 The particulate OC and an aSi rain rate were much lower than the recycling and burial fluxes
200 (Table 1). The OC/aSi molar ratio of the rain rate was 1-2, a much lower value than the measured
201 burial ratio (≈7, Table 1) which was consistent with deep-sea sediment and trap particles OC/aSi
202 ratio (Ragueneau et al., 2002).

203

204 **4 Discussion: Budgets, burial efficiencies and comparison to riverine and marine sources**

205 The striking point of these OC and aSi budgets is the high burial rates (0.35 Tg C $y^{-1}$ and 0.11 Tg
206 Si $y^{-1}$) and the large burial efficiencies (70-85%) compared to abyssal plain sediments, where
207 generally only <10% of the OC and aSi rain rates are buried (Burdige, 2007; Ragueneau et al.,
208 2002). In addition, the strong decoupling from the vertical marine flux (1% and 4% of the total
209 OC and aSi input, Table 2) is clear. Previous results have highlighted the terrestrial nature of the
210 lobe complex organic matter (Baudin et al., 2017b; Schnyder et al., 2017; Stetten et al., 2015).
211 The small contribution of marine inputs to the total input corroborates the dominance of canyon
212 inputs to the lobe complex. The comparison of the OC/aSi signature of the buried particulate
213 matter (7.1) to the two possible sources of material (riverine=13 and marine=1.5) also points to
214 the Congo River as the main source of sediments in the lobe complex, with limited decoupling
215 between carbon and silicon during the transfer of particles to the terminal lobes. The OC/aSi
216 decrease of riverine material from 13 to 7 can probably be attributed to preferential recycling of
217 carbon versus silica (Ragueneau et al., 2002) in surficial sediments before burial (Raimonet et

al., 2015). Overall, the rapid transfer of Si and C through the canyon leads to an enhanced preservation of Si and C with little decoupling (Raimonet et al., 2015) compared to the strong decoupling occurring during particle settling in the open ocean (Ragueneau et al., 2002). If generalized during glacial periods, this rapid transfer to the deep sea fans through the canyons, may lead to a decrease of biogenic matter deposition and recycling on continental shelves and slopes with the following consequences: long-term decrease of $CO_2$ production during mineralization of the organic matter, and short term changes of phytoplankton dynamics (diatoms) linked to lower silicic acid recycling from shelves and slopes sediments.

The present estimate of OC inputs to the lobe complex (0.42 Tg C $y^{-1}$) can be compared with recent estimates of canyon particulate export rates (0.5-1.1 Tg C $y^{-1}$ ) based on ADCP measurements of canyon turbidity currents at 2000 m water depth, 500 km upstream from the lobe complex (Azpiroz-Zabala et al., 2017). These comparable export rates between two distant sites indicates that the sediment transport along the canyon and deep-sea channel is very efficient and that a significant fraction (up to 50%) of the material transported by turbidity currents may reach the lobe complex located at the far end of the channel-levee system.

The Congo lobe complex represents an overlooked sink for organic carbon and amorphous silica in the abyssal Atlantic Ocean. The OC and aSi budgets in the lobe complex are dominated by burial fluxes, 3-4 orders of magnitude larger than those in the surrounding abyssal plain (38-1560 versus 0.06 g C $m^{-2}$ $y^{-1}$ and 11-381 versus 0.15 g Si $m^{-2}$ $y^{-1}$). When compared to the overall burial of OC in the South Atlantic (0-40°S) during the Holocene (Mollenhauer et al., 2004), the accumulation of OC in Congo terminal lobe sediments adds 19% to the estimation of OC burial in this deep ocean basin. This contribution is remarkable given the lobe area represents less than

0.01% of the South Atlantic surface area (0-40°S) and indicates that the Congo lobe complex constitutes a megasink of OC in the South Atlantic which was clearly overlooked in previous studies due to the lack of knowledge on Congo terminal lobes. Although slightly less acute, 3% of the total burial of aSi in the South Atlantic occurs in the lobe complex. This number could be raised to 4-6% if aSi was underestimated as suggested by Rahman et al. (2016). Burial fluxes of this dominantly terrestrial OC (70-90%; Schnyder et al., 2017; Stetten et al., 2015) and aSi, that represent 18% and 35% of the Congo River discharge of POC and aSi, respectively, are in the same range of estimates for deltaic sediments, i.e. 22% of river OC input preserved (Burdige, 2005; Hedges and Keil, 1995). The estimated burial of terrigenous OC in the lobe complex (0.3 Tg C $y^{-1}$) represents about 0.7% of the overall terrestrial OC burial in the global abyssal ocean (Schlünz and Schneider, 2000).

The present-day export to the abyssal depth of Congo River sediments through the presently active connection to its canyon, and therefore of embedded OC and aSi, is similar to the lowstand functioning of major deep-sea fans (Vail et al., 1977), e.g. Amazon fan (Flood and Piper, 1997). It may therefore be a representative glacial analogue for terrestrial OC and aSi export when rivers discharged at the shelf break and active canyons carried a large proportion of their load to the continental rise and abyssal plain (Schlünz et al., 1999). If, as suggested in previous studies (Burdige, 2005), the same fraction of the carbon load (18%) of other major tropical rivers of the Atlantic such as the Amazon (5 Tg C $y^{-1}$; Moreira-Turcq et al., 2003) or the Orinoco Rivers (1 Tg C $y^{-1}$; Mora et al., 2014) was buried in the deep Atlantic basin during glacial times, this burial flux would equal the present-day carbon preservation in the entire South Atlantic basin and significantly increase the global oceanic carbon sink during these low $CO_2$ periods. The OC burial estimate for the Amazon fan during glacial times (3.7 Tg C/yr; Schlünz et

al., 1999) clearly substantiate this calculation. These megasinks may also contribute to enhance OC storage during glacial by better preservation (burial efficiencies of 85%, Table 2) as proposed by Cartapanis et al. (2016). These findings emphasize the need to better constrain these localized but intense megasinks in order to understand the natural sinks in the carbon and silica cycles during both modern and glacial times.

## 5 Conclusions

In this paper, we have shown that the terminal lobes of the Congo deep-sea fan constitute a singular point in the South Atlantic Ocean corresponding to a mega burial site for organic carbon and amorphous silica. It represents 19% of the entire burial of the South Atlantic Ocean for OC despite covering less than 0.01‰ of the total surface area. By comparing burial in lobe sediments with the Congo River input, we conclude that 18% of organic carbon inputs and 35% of amorphous silica inputs from the Congo River are buried in sediments, which thus constitutes a major repository for exported riverine material. This is largely due to the present and active connection of the Congo canyon to the River estuary. This situation may represent a fair analogue to glacial period river export when most rivers were closely connected to their canyons due to the low sea level. It is expected that burial of OC and aSi in these terminal lobe regions of other rivers was much larger at this period.

## Conflict of interest

The authors state that there are no real or perceived conflicts of interests neither financial nor institutional.

## Data

Original data were all published with the original papers (see references in text) or are contained in the Supplementary Material. The entire dataset is currently being deposited in the SEANOE data base (IFREMER).


## Acknowledgments

The authors thank the captains and crews of the RV Pourquoi Pas? And the ROV teams during the WACS and Congolobe cruises. We thank two external reviewers (D. Conley, J.E. Cloern) who kindly provided useful comments to this paper. We acknowledge funding from ANR Congolobe (ANR Blanc SIMI5-6, no.11BS56030), from IFREMER (Project "Biodiversité et dynamique des écosystèmes profonds, impacts"), from CEA through LSCE (to CR) and from the U.S. National Science Foundation Chemical Oceanography Program (OCE-0831156 to MT).


## References


Allin, J. R., Hunt, J. E., Clare, M. A., & Talling, P. J. (2017). Eustatic sea-level controls on the flushing of a shelf-incising submarine canyon, *GSA Bulletin*, *130*, 222-237, doi: https://doi.org/10.1130/B31658.1.

Azpiroz-Zabala, M., Cartigny, M. J. B., Talling, P. J., Parsons, D. R., Summer, E. J., Clare, M. A., Simmons, S. M., Cooper, C., & Pope, E. L. (2017). Newly recognized turbidity current structure can explain prolonged flushing of submarine canyons, *Sci. Adv.*, *3*, e1700200, doi: 10.1126/sciadv.1700200.

Babonneau, N., Savoye, B., Cremer, M., & Klein, B. (2002). Morphology and architecture of the present canyon and channel system of the Zaire dees-sea fan, *Mar. Petrol. Geol.*, *19*, 445-467.

Battin, T. J., Luyssaert, S., Kaplan, L. A., Aufdenkampe, A. K., Richter, A., & Tranvik, L. J. (2009). The boundless carbon cycle, *Nature Geoscience*, *2*, 598-600.

Baudin, F., Martinez, P., Dennielou, B., Charlier, K., Marsset, T., Droz, L., & Rabouille, C. (2017a). Organic carbon accumulation in modern sediments of the Angola basin influenced by the Congo deep sea fan, *Deep-Sea Res. II: Top. Stud. Oceanorgr.*, *142*, 64-74.

Baudin, F., Stetten, E., Schnyder, J., Charlier, K., Martinez, P., Dennielou, B., & Droz, L. (2017b). Origin and distribution of the organic matter in the distal lobe of the Congo deep-sea fan – A Rock-Eval survey, *Deep-Sea Res. II: Top. Stud. Oceanorgr.*, *142*, 75-90.

Bauer, J. E., Cai, W. J., Raymond, P. A., Bianchi, S. T., Hopkinson, C. S., & Regnier, P. A. G. (2013). The changing carbon cycle of the coastal ocean, *Nature*, *504*, 61-70.

Berner, R. A. (1989). Biogeochemical cycles of carbon and sulfur and their effect on atmospheric oxygen over phanearozoic time, *Pal. Pal. Pal.*, *73*, 97-122.

317 Bianchi, S. T., & Allison, M. A. (2009). Large-river delta-front estuaries as natural ‘‘recorders’’ of global
318 environmental change, *Proc. Nat. Acad. Sci.*, *106*, 8085–8092.
319 Bianchi, S. T., Allison, M. A., & Cai, W. J. (2014), Biogeochemical dynamics at major river-coastal interfaces:
320 linkages with Global Change, 649 pp., Cambridge University Press, New York.
321 Blair, N. E., & Aller, R. C. (2012). The fate of terrestrial organic carbon in the marine environment, *Ann. Rev. Mar.*
322 *Sci.*, *4*, 401-423, doi: doi.org/10.1146/annurev-marine-120709-142717. .
323 Bouma, A. H., Coleman, J. H., Stelting, C. E., & Kohl, B. (1989). Influence of relative sea level changes on the
324 construction of the Mississippi fan, *Geo-Marine Letters*, *93*, 161-170, doi: https://doi.org/10.1007/BF02431043.
325 Burdige, D. J. (2005). Burial of terrestrial organic matter in marine sediments: A re-assessment, *Glob. Biogeochem.*
326 *Cycles*, *19*, GB4011, doi: doi:10.1029/2004GB002368.
327 Burdige, D. J. (2006), Geochemistry of marine sediments, 609 pp., Princeton University Press, Princeton, USA.
328 Burdige, D. J. (2007). Preservation of Organic Matter in Marine Sediments: Controls, Mechanisms and an
329 Imbalance in Sediment Organic Carbon Budgets?, *Chem. Rev.*, *107*, 467-485, doi:
330 http://dx.doi.org/10.1021/cr050347q.
331 Canals, M., Puig, P., Durrieu de Madron, X., Heussner, S., Palanques, A., & Fabres, J. (2006). Flushing submarine
332 canyons, *Nature*, *444*, doi:10.1038/nature05271.
333 Cartapanis, O., Bianchi, D., Jaccard, S.L. and Galbraith, E.D. (2015) Global pulses of organic carbon burial in deep-
334 sea sediments during glacial maxima. Nature Comm. 7:10796.
335 Congolobe group, et al. (2017). The Congolobe project, a multidisciplinary study of Congo deep-sea fan lobe
336 complex: Overview of methods, strategies, observations and sampling, *Deep-Sea Res. (II) Topic. Stud. in*
337 *Oceanogr.*, *142*(7-24).
338 Constantinescu, A. M., Toucanne, S., Dennielou, B., Jorry, S. J., Mulder, T., & Lericolais, G. (2015). Evolution of
339 the danube deep-sea fan since the last glacial maximum: New insights into Black Sea water-level fluctuations,
340 *Mar. Geol.*, *367*, 50-68, doi: http://dx.doi.org/10.1016/j.margeo.2015.05.007.
341 Covault, J. A., & Graham, S. A. (2010). Submarine fans at all sea-level stands: Tectono-morphologic and climatic
342 controls on terrigenous sediment delivery to the deep sea, *Geology*, *38*, 939-942, doi:
343 https://doi.org/10.1130/G31081.1.
344 Covault, J. A., & Fildani, A. (2014), Continental shelves as sediment capacitors or conveyors: source-to-sink
345 insights from the tectonically active Oceanside shelf, southern California, USA, edited, p. 315, Geological
346 Society of London Memoirs.
347 Cox, P. M., Betts, R. A., Jones, C. D., Spall, S. A., & Totterdell, I. J. (2000). Acceleration of global warming due to
348 carbon-cycle feedbacks in a coupled climate model, *Nature*, *408*, 184-187.
349 Demaster, D. J. (2002). The accumulation and cycling of biogenic silica in the Southern Ocean: revisiting the marine
350 silica budget, *Deep-Sea Research II*, *49*, 3155-3167.
351 Dennielou, B., et al. (2017). Morphology, structure, composition and build-up processes of the active Congo
352 channel-mouth lobe complex with inputs from remotely operated underwater vehicle (ROV) multibeam and
353 video surveys, *Deep-Sea Res. (II): Top. Stud.Oceanogr.*, *142*, 25-49.
354 Flood, R. D., & Piper, D. J. W. (1997). Amazon fan sedimentation: the relationship to equatorial climate change,
355 continental denudation, and sea-level fluctuations, *Proceedings of the Ocean Drilling Program, Scientific*
356 *Results*, *155*, 653-675.
357 Frank, D. C., Esper, J., Raible, C. C., Buntgen, U., Trouet, V., Stocker, B., & Joos, F. (2010). Ensemble
358 reconstruction constraints on the global carbon cycle sensitivity to climate, *Nature*, *463*, 527-230, doi:
359 doi:10.1038/nature08769.
360 Geibert, W., Rutgers van Der Loeff, M. M., Usbeck, R., Gersonde, R., Kuhn, G., & Seeberg-Everfeldt, J. (2005).
361 Quantifying the opal belt in the Atlantic and southeast Pacific sector of the Southern Ocean by means of 230Th
362 normalization, *Glob. Biogeochem. Cycle*, *19*, GB4001, doi: doi:10.1029/2005GB002465.
363 Goni, M. A. (1997), Records of terrestrial organic matter composition in Amazon Fan sediments in Proceedings of
364 the Ocean Drilling Program-Scientific Results, edited by R. D. Flood, D. J. W. Piper and L. C. Peterson, pp. 519-
365 530, Ocean Drill. Program, College Station, Tex.
366 Hedges, J. I., & Keil, R. G. (1995). Sedimentary organic matter preservation: an assessment and speculative
367 synthesis, *Mar. Chem.*, *49*, 81-115.
368 Heezen, B. C., Menzies, R. J., Schneider, E. D., Ewing, W. M., & Granelli, N. C. L. (1964). Congo Submarine
369 Canyon, *AAPG Bulletin*, *48*, 1126–1149.
370 Keil, R. G., Tsamakis, E. C., Wolf, N., Hedges, J. I., & Goni, M. A. (1997), Relationships between organic carbon
371 preservation and mineral surface area in Amazon Fan sediments (Holes 932A and 942A), in Proceedings of the

Ocean Drilling Program-Scientific Results, edited by R. D. Flood, D. J. W. Piper and L. C. Peterson, pp. 531-538, Ocean Drill. Program, College Station, Tex.
Khripounoff, A., Caprais, J., Crassous, P., & Etoubeau, J. (2006). Geochemical and biological recovery of the disturbed seafloor in polymetallic nodule fields of the Clipperton-Clarion Fracture Zone (CCFZ) at 5,000-m depth, *Limnol. Oceanogr.*, *51*, 2033-2041.
Khripounoff, A., Vangriesheim, A., Babonneau, N., Crassous, P., Savoye, B., & Dennielou, B. (2003). Direct observation of intense turbidity current activity in the Zaire submarine valley at 4000 m water depth, *Mar. Geol.*, *194*, 151-158.
Lansard, B., Rabouille, C., Denis, L., & Grenz, C. (2009). Benthic remineralization at the land-ocean interface: A case study of the Rhone River (NW Mediterranean Sea), *Estuarine Coastal and Shelf Science*, *81*(4), 544-554, doi: 10.1016/j.ecss.2008.11.025.
Laruelle, G. G., et al. (2009). Anthropogenic perturbations of the silicon cycle at the global scale: Key role of the land-ocean transition, *Glob. Biogeochem. Cycle*, *23*, GB4031, doi: doi:10.1029/2008GB003267.
Lombo Tombo, S., Dennielou, B., Berné, S., Bassetti, M. A., Toucanne, S., Jorry, S. J., Jouet, G., & Fontanier, C. (2015). Sea-level control on turbidite activity in the Rhone canyon and the upper fan during the Last Glacial Maximum and Early deglacial, *Sediment. Geol.*, *323*, 148-166, doi: http://dx.doi.org/10.1016/j.sedgeo.2015.04.009.
Milliman, J. D. (1991), Flux and fate of fluvial sediment and water in coastal seas, in Ocean margin processes in global change, edited by R. F. C. Mantoura, J-M. Martin and R. Wollast, pp. 69-91, J. Wiley and sons, Berlin.
Mollenhauer, G., Schneider, R. R., Jennerjahn, T., Muller, P. J., & Wefer, G. (2004). Organic carbon accumulation in the South Atlantic Ocean: its modern, mid-Holocene and last glacial distribution, *Glob. Planet. Change*, *40*, 249-266.
Mora, A., Laraque, A., Moreira-Turcq, P., & Alfonso, J. A. (2014). Temporal variation and fluxes of dissolved and particulate organic carbon in the Apure, Caura and Orinoco rivers, Venezuela, *South Amer. J. Earth Sci.* , *54*, 47-56, doi: http://dx.doi.org/10.1016/j.jsames.2014.04.010.
Moreira-Turcq, P., Seyler, P., Guyot, J. L., & Etcheber, H. (2003). Exportation of organic carbon from the Amazon River and its main tributaries, *Hydrol. Process.*, *17*, 1329–1344, doi: DOI: 10.1002/hyp.1287.
Mulder, T., & Etienne, S. (2010). Lobes in deep-sea turbidite systems: State of the art, *Sediment. Geol.*, *229*, 75-80, doi: 10.1016/j.sedgeo.2010.06.011.
Newman, J. W., Parker, P. L., & Behrens, E. W. (1973). Organic carbon ratios in Quaternary cores from the Gulf of Mexico, *Geochim. Cosmochim. Acta*, *37*, 225– 238.
Olu, K. (2011). WACS cruise, R/V Pourquoi Pas?, doi: http://dx.doi.org/10.17600/11030010.
Olu, K., Decker, C., Pastor, L., Caprais, J. C., Khripounoff, A., Morineaux, M., Ain Baziz, M., Menot, L., & Rabouille, C. (2017). Cold-seep-like macrofaunal communities in organic- and sulfide-rich sediments of the Congo deep-sea fan, *Deep-Sea Res. (II) Topic. Stud. in Oceanogr.*, *142*, 180-196.
Parrenin, F., Masson-Delmotte, V., Kohler, P., Raynaud, D., Paillard, D., Schwander, J., Barbante, C., Landais, A., Wegner, A., & Jouzel, J. (2013). Synchronous change of atmospheric $CO_2$ and antarctic temperature during the last deglacial warming, *Science*, *339*, 1060-1063, doi: DOI: 10.1126/science.1226368.
Picot, M. (2015), Cycles sédimentaires dans le système turbiditique du Congo: nature et origine (Doctorat Thesis). Université de Bretagne Occidentale, Brest, 368., 368 p pp, Université de Bretagne Occidentale, Brest.
Posamentier, H. W., & Vail, P. R. (1988), Eustatic Controls on Clastic Deposition II—Sequence and Systems Tract Models, in Sea-Level Changes: An Integrated Approach, edited by C. K. W. e. al., SEPM Society for Sedimentary Geology,.
Rabouille, C. (2011). CONGOLOBE cruise, R/V Pourquoi Pas? , doi: http://dx.doi.org/10.17600/11030170.
Rabouille, C., Mackenzie, F., & Ver, L. M. (2001). Influence of the human perturbation on carbon, nitrogen and oxygen biogeochemical cycles in the global coastal ocean, *Geochim. Cosmochim. Acta*, *65*, 3615-3639.
Rabouille, C., Caprais, J. C., Lansard, B., Crassous, P., Dedieu, K., Reyss, J. L., & Khripounoff, A. (2009). Organic matter budget in the Southeast Atlantic continental margin close to the Congo Canyon: In situ measurements of sediment oxygen consumption, *Deep-Sea Research Part Ii-Topical Studies in Oceanography*, *56*(23), 2223-2238, doi: 10.1016/j.dsr2.2009.04.005.
Ragueneau, O., Dittert, N., Pondaven, P., Treguer, P., & Corrin, L. (2002). Si/C decoupling in the world ocean : is the Southern Ocean different?, *Deep-Sea Res. II*, *49*, 3127-3154.
Ragueneau, O., Regaudie-de-Gioux, A., Moriceau, B., Gallinari, M., Vangriesheim, A., Baurand, F., & Khripounoff, A. (2009). A benthic Si mass balance on the Congo margin: Origin of the 4000 m DSi anomaly and implications for the transfer of Si from land to ocean, *Deep Sea Research Part II: Topical Studies in Oceanography*, *56*(23), 2197.

Raimonet, M., Ragueneau, O., Jacques, V., Corvaisier, R., Moriceau, B., Khripounoff, A., Pozzato, L., & Rabouille, C. (2015). Rapid transport and high accumulation of amorphous silica in the Congo deep-sea fan: a preliminary budget, *J. Mar Sys.*, *141*, 71-79.

Regnier, P. A. G., et al. (2013). Anthropogenic perturbation of the carbon fluxes from land to ocean, *Nat. Geosc.*, *6*, 597-607, doi: DOI: 10.1038/NGEO1830.

Savoye, B., Babonneau, N., Dennielou, B., & Bez, M. (2009). Geological overview of the Angola-Congo margin, the Congo deep-sea fan and its submarine valleys, *Deep Sea Research Part II: Topical Studies in Oceanography*, *56*(23), 2169.

Schlünz, B., & Schneider, R. R. (2000). Transport and terrestrial organic carbon to the oceans by rivers: re-estimating flux and burial rates, *Int. J. Earth Sci.*, *88*, 599-606.

Schlünz, B., Schneider, E. D., Muller, P. J., Showers, W. J., & Wefer, G. (1999). Terrestrial organic carbon accumulation on the Amazon deep sea fan during the last glacial sea level low stand, *Chem. Geol.*, *159*, 263–281.

Schnyder, J., Stetten, E., Baudin, F., Pruski, A., & Martinez, P. (2017). Palynofacies reveal fresh terrestrial organic matter inputs in the terminal lobes of the Congo deep-sea fan, *Deep-Sea Res. (II) Topic. Stud. in Oceanogr.*, *142*, 91-108.

Shanmugam, G., & Moiola, R. J. (1982). Eustatic control of turbidites and winnowed turbidites, *Geology*, *10*, 231-235, doi: https://doi.org/10.1130/0091-7613(1982)10<231:ECOTAW>2.0.CO;2.

Spencer, R. G. M., Stubbins, A., & Gaillardet, J. (2014), Geochemistry of the Congo River, estuary and plume, in Biogeochemical dynamics at the major river-coastal interfaces, edited by S. T. Bianchi, M. A. Allison and W. J. Cai, pp. 554-606, Cambridge Univ. Press, New York.

Stetten, E., Baudin, F., Reyss, J. L., Martinez, P., Charlier, K., Schnyder, J., Rabouille, C., Dennielou, B., Coston-Guarini, J., & Pruski, A. (2015). Organic matter characterization and distribution in sediments of the terminal lobes of the Congo deep-sea fan: evidence for the direct influence of the Congo River, *Mar. Geol.*, *369*, 182-195.

Tréguer, P., & De La Rocha, C. L. (2013). The world ocean silica cycle, *Ann. Rev. Mar. Sci.*, *5*, 477–501, doi: 10.1146/annurev-marine-121211-172346.

Tréguer, P., et al. (2018). Influence of diatom diversity on the ocean biological carbon pump, *Nat. Geosc.*, *11*, 27–37, doi: doi/10.1038/s41561-017-0028-x.

Tsandev, I., Rabouille, C., Slomp, C. P., & Van Cappellen, P. (2010). Shelf erosion and submarine river canyons: implications for deep-sea oxygenation and ocean productivity during glaciation, *Biogeosciences*, *7*(6), 1973-1982, doi: 10.5194/bg-7-1973-2010.

Vail, P. R., Mitchum, R. M., Todd, R. G., Widmier, J. M., Thompson III, S., Sangree, J. B., Bubb, J. N., & Hatelid, W. G. (1977), Seismic stratigraphy and global changes of sea level, in Seismic stratigraphy—Applications to hydrocarbon exploration, edited by C. E. Payton, pp. 49-212, American Association of Petroleum Geologists Memoir,.

Van Cappellen, P., & Wang, Y. (1996). Cycling of iron and manganese in surface sediments: a general theory for the coupled transport and reaction of carbon, oxygen, nitrogen, sulfur, iron and manganese, *Amer. J. Sci.*, *296*, 197-243.

Vangriesheim, A., Khripounoff, A., & Crassous, P. (2009). Turbidity events observed in situ along the Congo submarine channel, *Deep-Sea Res. II*, doi:10.1016/j.dsr1012.2009.1004.1004

Wenzhöfer, F., & Glud, R. N. (2002). Benthic carbon mineralization in the Atlantic: A synthesis based on in situ data from the last decade, *Deep-Sea Res. (I)*, *49*, 1255-1279.

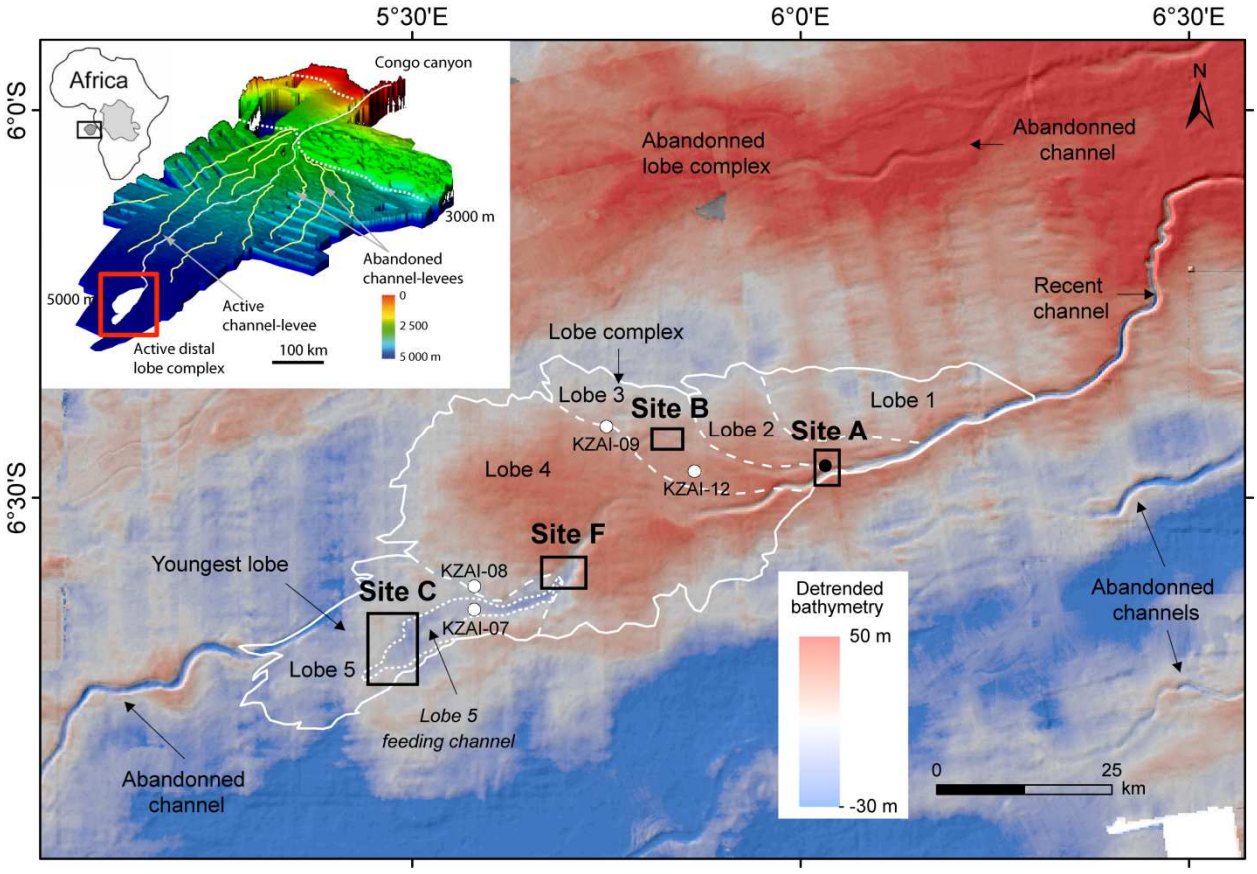


***Fig.1:*** *Map and high resolution detrended bathymetry of the terminal lobes of the Congo deep-sea fan showing the contours of lobes numbered from 1 to 5 according to their distance from the entrance of the lobe complex (=recent channel). Average depth is 4800m (Congolobe group, 2017). Stations were located at four representative sites along the lobes (A=Lobe 1+Lobe 2, B=Lobe 3, F=Lobe 4, C=Lobe 5). The dotted line contour outlines the lobe 5 feeding channel that shows the highest sedimentation rates. White dots show the location of sediment cores used for additional sedimentation rate calculation. The black dot on Site A shows the location of sediment traps deployed in 2011.*

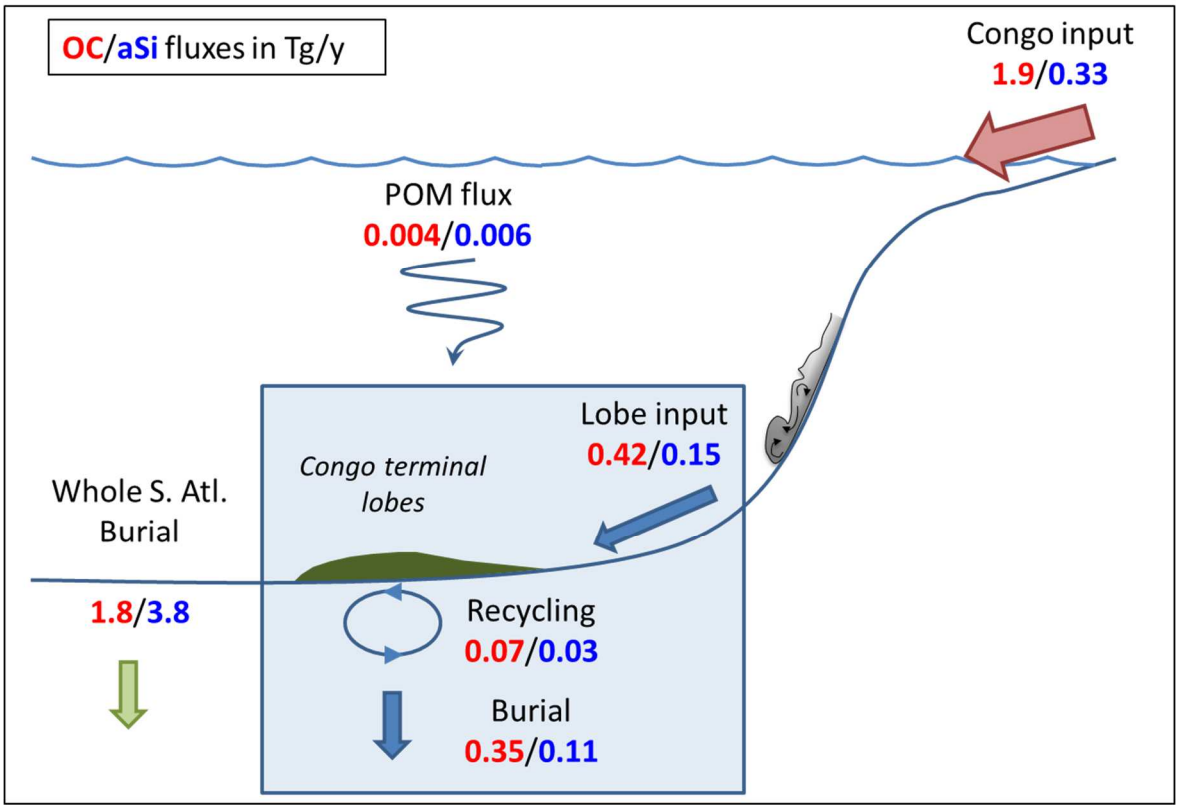


***Figure 2:*** *Mass balance for the Congo terminal lobe complex for organic carbon (OC in Tg C $y^{-1}$; 1 Tg = $10^{12}$ g) and amorphous silica (aSi in Tg Si $y^{-1}$). Input from the Congo River, from the marine rain and burial rates in the South Atlantic basin (0-40°S) are also displayed. Red numbers are for OC and blue for aSi.*

**Table 1**: *Recycling, burial and vertical fluxes for OC and aSi in Congo lobe sediments. Recycling fluxes of OC (mineralization) and aSi (dissolution) was calculated from TOU (total oxygen uptake) and DSi flux (dissolved silica flux). Conversion of TOU to OC mineralization was made using a molar ratio C/$O_2$ of 0.9 (see text). Burial fluxes were calculated from measured sedimentation rates, porosity and average OC and aSi content of surface sediments (0-20cm). For recycling and burial, a weighted average for the entire lobe complex was calculated using the proportion of surface area of each lobe (see below). The measured porosity values were averaged for depth in core between 10 and 40 cm. Vertical fluxes are from station A (unpublished when unmarked). The mark (*) values are from Rabouille et al. (2009) and Ragueneau et al. (2009) measured at site Bio-D 200km East of the Lobe zone at 400m above seafloor.*

| | Site A (Lobes1&2) | Site B (Lobe 3) | Site F (Lobe 4) | Site C levee (Lobe 5) | Site C channel (Lobe 5 feeding channel) | Weighted average |
|---|---|---|---|---|---|---|
| **Recycling** | | | | | | |
| Surface area ($km^2$) | 533 | 283 | 1203 | 424 | 82 | |
| TOU (mmol $O_2$ $m^{-2}$ $d^{-1}$) | 5.4±0.5 | 7±0.9 | 6.5±0.7 | 7.8±0.4 | 9.6±0.8 | |
| OC miner (g C $m^{-2}$ $y^{-1}$) | 21±2 | 28±4 | 26±3 | 31±2 | 38±4 | **26±4** |
| DSi flux (mmol Si $m^{-2}$ $d^{-1}$) | 1.1±0.1 | - | 1.9±0.2 | 0.6±0.1 | 0.6±0.1 | |
| aSi dissol. (g Si $m^{-2}$ $y^{-1}$) | 7.7±0.7 | - | 19±2 | 6.2±0.6 | 5.9±0.6 | **13±2** |
| **Burial** | | | | | | |
| Sedim. rate (cm $y^{-1}$) | 1±0.3 | 0.3±0.1 | 0.7±0.2 | 0.7±0.2 | 12±6 | |
| Porosity | 0.84 | 0.84 | 0.85 | 0.85 | 0.87 | |
| OC (% dw) | 3.25±0.2 | 3.2±0.2 | 3.3±0.2 | 3.4±0.2 | 4.0±0.2 | |
| aSi (%Si dw) | 1.3±0.1 | 0.9±0.1 | 1.2±0.1 | 1.2±0.1 | 1.0±0.1 | |
| OC Burial (g C $m^{-2}$ $y^{-1}$) | 130±40 | 38±12 | 87±30 | 89±32 | 1560±540 | **139±42** |
| aSi Burial (g Si $m^{-2}$ $y^{-1}$) | 53±11 | 11±4 | 32±8 | 31±9 | 381±125 | **45±11** |
| OC/aSi burial (mol/mol) | 5.8 | 8.0 | 6.3 | 6.7 | 9.6 | **7.1** |
| **Vertical flux** | | | | | | |
| F-aSi (g Si $m^{-2}$ $y^{-1}$) | 1.5-2.5* | | | | | |
| F-OC (g C $m^{-2}$ $y^{-1}$) | 1.1-1.7* | | | | | |

**Table 2**: *Mass balance for the terminal lobes of the Congo deep-sea fan and comparison to the marine particulate fluxes, Congo discharge and burial in the South Atlantic (1 Tg = $10^{12}$ g). *aSi burial in the South Atlantic is calculated from the regional organic carbon burial and OC/aSi ratio or downscaling global fluxes (see supplementary material). OC/aSi is calculated as molar ratio compared to mass fluxes for OC and aSi.*

| | OC (Tg C $y^{-1}$) | aSi (Tg Si $y^{-1}$) | OC/aSi (mol/mol) |
|---|---|---|---|
| Burial | 0.35 ± 0.12 | 0.11 ± 0.05 | 7.1 |
| Mineralization/dissolution | 0.07 ± 0.01 | 0.03 ± 0.01 | |
| **Lobe input based on mass balance** | **0.42 ± 0.14** | **0.15 ± 0.05** | **8.0** |
| Burial efficiency (BE) | 84% | 73% | |
| Marine input | 0.004 | 0.006 | 1.5 |
| % marine in total input | 1% | 4% | |
| River discharge (Coynel et al., 2005; Hugues et al., 2011; Seylers et al., 2005) | 1.9 | 0.33 | 13 |
| % burial of Congo River export | 18% | 35% | |
| Burial in deep South Atlantic (0-40°S; >3000m; (Mollenhauer et al., 2004) | 1.8 | 3.8* | 1 |
| % burial in Congo lobes relative to deep South Atlantic | 19% | 3% | |